# Measurements of Turbulent Boundary Layer Prandtl Numbers and Space-time Temperature Correlations

Nader Bagheri,* Constantine J. Strataridakis,* and Bruce R. White†
*University of California, Davis, Davis, California 95616*

**Hot-wire anemometry measurements in an incompressible turbulent boundary-layer flow over a heated flat plate at zero pressure gradient were made using an $x$ probe and a temperature fluctuation probe. The measurements were made for three different temperature difference cases between the wall and the freestream 10, 15, and 20° C. Simultaneous measurements of the two components of the velocity and the temperature were made at the same point using an $x$ probe and a temperature fluctuation probe. The experiments resulted in direct measurement of the turbulent Prandtl number as a function of height through the boundary layer for the three temperature difference cases. Also, space-time correlations of temperature fluctuations $T'$ were obtained with a pair of temperature fluctuation probes. The mean convection velocities of the $T'$ large-scale structure are presented for the three temperature difference-cases. The mean convection velocity of the $T'$ structure is a function of position $y^+$ and was found to be independent of the temperature difference for the cases considered. The convection velocity varied from $0.65_\infty$ at the smallest measured value of $y^+ = 75$ to about $0.77u_\infty$ at $y^+ = 425$, the largest measured value of $y^+$.**

## Nomenclature

$C_p$ = heat capacity at constant pressure
$k$ = thermal conductivity
$Pr$ = Prandtl number
$Pr_t$ = turbulent Prandtl number
$q''$ = heat flux
$Re_\theta$ = Reynolds number, $U_\infty\theta/\nu$
$R_{T,T}$ = cross-correlation temperature coefficient
$T$ = temperature
$T^*$ = friction temperature, $q_w''/(\rho C_p u^*)$
$t$ = time
$U$ = time-mean average streamwise velocity
$u$ = instantaneous streamwise velocity
$u^*$ = friction velocity
$v$ = instantaneous normal velocity
$x$ = streamwise direction
$y$ = normal direction
$z$ = spanwise direction
$\delta$ = hydrodynamic boundary-layer thickness
$\delta_t$ = thermal boundary-layer thickness
$\epsilon_H$ = eddy conductivity of heat
$\epsilon_M$ = eddy viscosity of momentum
$\nu$ = kinematic viscosity
$\rho$ = density
$\tau$ = shear stress
$\theta$ = momentum thickness
$\Delta_2$ = enthalpy thickness

*Subscripts*

$\infty$ = freestream
$c$ = convection
$t$ = turbulent
$w$ = wall

*Superscripts*

$'$ = fluctuating quantity
$+$ = normalization with viscous units

## Introduction

THE present study is an experimental investigation of a turbulent boundary layer developing over a heated flat plate. The characteristics and structure of the flow will be investigated through a series of space-time correlation measurements. It is hoped that this study would enhance our understanding of the physics of the heat transfer mechanism associated with the turbulent temperature structure in the near-wall region.

During the last decade, much attention has been given to the study of coherent structures in turbulent flows. Turbulence contains a collection of large-scale coherent structures that have dimensions comparable with the size of the boundary layer. The term large-scale structures conveys the notion that the coherent structures have significant correlation over a significant region of the boundary layer. Space-time correlation methods have, therefore, been used to investigate these large-scale coherent structures. It was first through flow visualization experiments that large-scale structures were observed. It was through the space-time correlation measurements that the existence of large-scale motions correlated with the shape and motion of the turbulent structures were confirmed. The large-scale motions were found to be three-dimensional and elongated in the streamwise direction, and the outer nonturbulent fluid appeared to be riding over the turbulent/nonturbulent interface.

Space-time correlation methods have been and continue to be an important tool in understanding the physics of the turbulent boundary layer. The time and length scales of turbulent flows may be estimated by means of such correlations. These scales are measures of temporal and spatial coherence of the turbulent flow structures, which are responsible for the bulk of the transport of momentum and heat.

The space-time correlation measurements of the velocity fluctuations for isothermal flows has been carried out by many investigators' measurements. Kline and Robinson[1] organized a community-wide survey and evaluation of coherent structures and motions in isothermal turbulent boundary layers. In their survey they defined the state of the turbulence structure knowledge. Recently Strataridakis, White, and Robinson[2] obtained the space-time correlation of the $u'$ and

Presented as Paper 90-0020 at the AIAA 28th Aerospace Sciences Meeting, Reno, NV, Jan. 8-11, 1990; received Feb. 2, 1990, revision received Sept. 4, 1990; accepted for publication Sept. 6, 1990. 

*Postgraduate Researcher, Department of Mechanical Engineering. Member AIAA.

†Professor, Department of Mechanical Engineering. Member AIAA.

$v'$ velocities and of their instantaneous product, using a pair of $x$ wire probes. From their results they obtained the mean convection velocities of the $u'$, $v'$, and $u'v'$ large-scale structures.

In this study, a two-dimensional turbulent boundary layer developing on a smooth heated surface in zero-pressure-gradient flow with an unheated starting length is investigated. The objective of the study is to make a detailed study of this flow, emphasizing the following objectives: 1) to make direct measurements of the turbulent $Pr$ number, and 2) to obtain two-point correlations to the temperature fluctuation measurements for the calculation of the mean convection velocity of the $T'$ large-scale structure.

## Experimental Facility

The experiments were carried out in an open-return type wind tunnel with an overall length of 7.5 m. The entrance section had a 13.6:1 contraction ratio with a bell-mouth shape. Air filter, Hexcel honeycomb, and six screens were placed at the entrance of the converging section in order to remove the dust particles, straighten the flow, and reduce the freestream turbulence level.

The test section of the tunnel was 3.04 m long, 0.304 m high, and 0.304 m wide. This section was designed to provide a zero-pressure-gradient environment. The freestream turbulence intensity in the section was less than 1.5%; the freestream velocity ranged from 2.5 to 25 m/s. Access to the test section was through four Plexiglas doors, two on each side of the test section. Each door was screwed to the test section at the four corners. Additional sealing was achieved by taping the Plexiglas doors to the test section from the sides.

The diffuser section was 2.26 m long and had an expansion area that provided a continuous transition from the rectangular cross-sectional area of the test section to a circular cross section of the fan. The converging and diffuser sections were both attached to the test section.

## Experimental Design

The phenomenon of heat transfer from a flat plate with a step change in surface temperature was selected to study the turbulent temperature structure in the near-wall region of the boundary layer. This phenomenon, with the velocity and temperature boundary layers, and the associated velocity and temperature profiles are illustrated in Fig. 1.

The flat plate consisted of an unheated starting length and a heated portion, thereby making the origins of momentum and thermal boundary layers different. The unheated starting

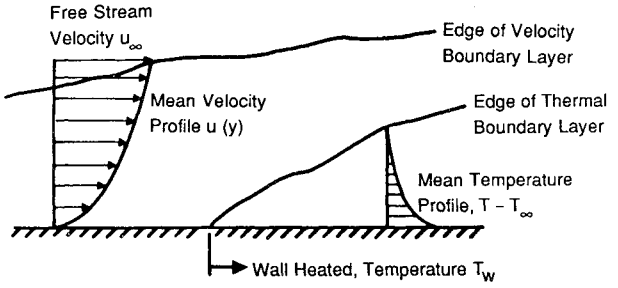


**Fig. 1 Velocity and temperature boundary layers and their associated profiles.**

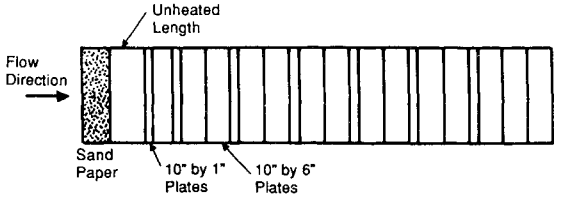


**Fig. 2 Wind-tunnel floor area in test section.**

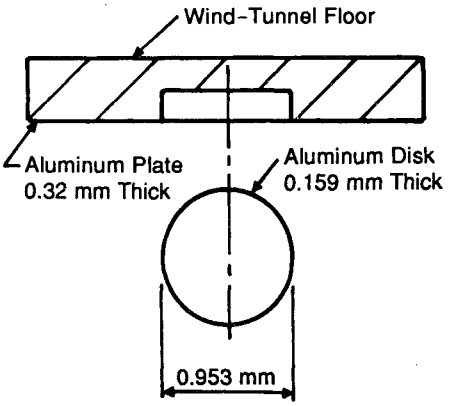


**Fig. 3 Cross section of an aluminum plate showing the location of an embedded thermocouple.**

length was 42.6 cm long with a leading-edge sand paper surface of 15.25 cm long for tripping the momentum boundary layer. The purpose of the unheated starting length was to confine the thermal layers within the hydrodynamic layer.

The heated portion of the flat plate consisted of 21 individually heated aluminum plates. These plates came in two different sizes: some 10 in. wide by 1 in. long, and the other 10 in. wide by 6 in. long. The plates were 0.125 in. thick, and were arranged as shown in Fig. 2. The plates were separated from each other by 0.125 in.-thick cork board, and the junctions were carefully mated to ensure an aerodynamically smooth surface through the entire length of the test section.

The plates were heated by silicon rubber heating elements. The size of the heating elements and its wattage density were especially manufactured to fit the plates and provide the required surface temperature. The power input to each plate was controlled by commercially available rhotostat switches.

The heating elements also came in two different sizes to fit the aluminum plates: some 10 in. wide by 1 in. long, and the others 10 in. wide by 6 in. long. The power input to the heating elements was calibrated against the root mean square voltage across the heating element. The current input to the plates were all drawn from a voltage regulator in order to supply a constant power to the plates for a given rhotostat switch setting. The heating elements were placed adjacent and beneath the aluminum plates.

The heating elements were insulated from the bottom using various insulating materials. The insulating materials used were fiberglass ($k = 0.0484$ $w/m \cdot K$), cork board ($k = 0.0433$ $w/m \cdot K$), and styrofoam ($k = 0.0381$ $w/m \cdot K$). The conduction and radiation heat losses from the bottom side of the plates for the three different temperature cases considered in this study were calculated and found to be small, a maximum of about 3% of the heat input to the plates.

The surface temperature of the aluminum plates was measured using type E miniature thermocouples, having a diameter of 0.127 mm. Figure 3 shows the model used in this study for surface temperature measurements. In this model, circular cavities 0.159 mm deep and 0.953 mm in diameter were milled in the aluminum plates, and the thermocouples were then placed in the cavities. The thermocouples came to direct contact with the aluminum plates by placing the aluminum disks, made to fit the cavities, inside the cavities. The advantages of this model are to eliminate natural convection and radiation losses and to minimize the introduction of foreign materials between the thermocouples and the solid surface.[3] With minor exceptions three thermocouples were embedded in each of the aluminum plates, one at the center and two at the opposite lateral ends. The two lateral end points were positioned a distance of $\pm 8.25$ cm from the center.

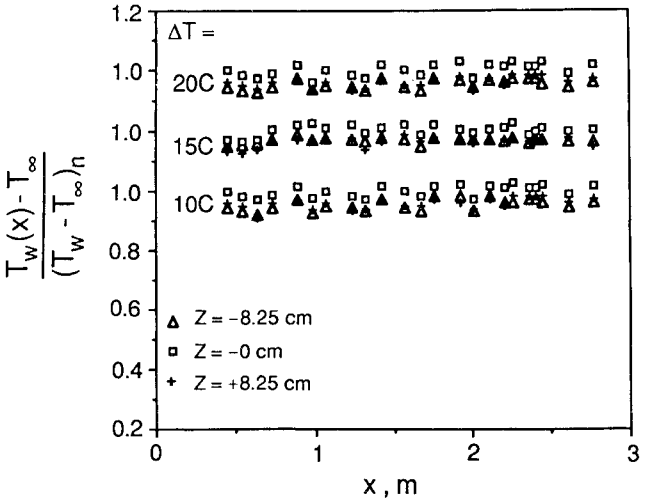


Fig. 4a Wall-temperature distributions.

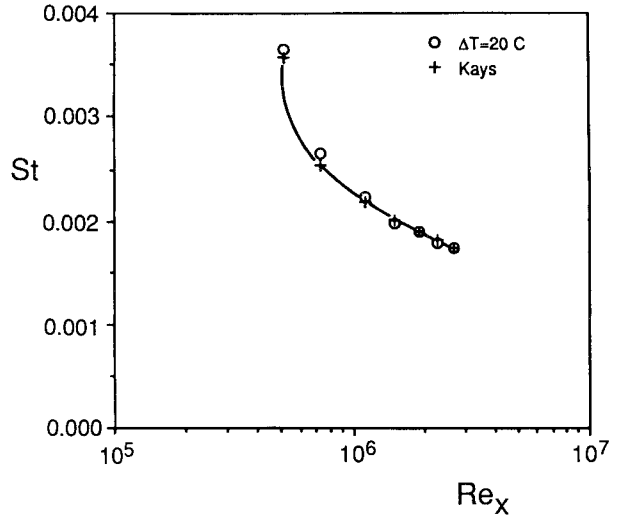


Fig. 4b Stanton number distribution.

The wall-temperature distributions for the 10, 15, and 20° C temperature cases are shown in Fig. 4a. The figure contains three wall-temperature distributions, for each temperature difference case, which correspond to the three different spanwise positions. The wall temperatures were normalized with respect to the nominal temperature difference at the center line location and show acceptable uniformity along plate. For the 10, 15, and 20° C temperature difference cases, the wall temperatures were uniform within ±0.2, ±0.25, and ±0.35° C, respectively.

Values of the thermal boundary-layer thicknesses of the three temperature difference cases and the hydrodynamic boundary-layer thicknesses are listed in Table 1. Temperature measurements at various downstream locations show that the thermal layers are normal, mature, and two dimensional. The evolution of the thermal layer along the plate is normal. This is shown in a plot of Stanton number vs $Re_x$ (Fig. 4b) for a typical temperature difference case. The thermal mixing parameter $k_h$ was equal to 0.4 at the measurement station for a value of enthalpy thickness Reynolds number of 3770.

Initially it was feared that the 1/8 in. cork boards might cause a thermal restart condition, thus creating a deviation in the Stanton number distribution as a function of downstream distance. The good agreement between this experiment and the empirical equation of Kays shown in Fig. 4b confirms that the minor thermal restart condition created by the cork boards is not a major problem.

The 1.5% freestream turbulence probably caused a minor increase in the surface heat flux. However, the effect of freestream turbulence, although always present, does not significantly increase Stanton number until the turbulence level exceeds 2%.[4] Figure 7 of Blair's work shows that only noticeable deviation in the Stanton number distribution results when the freestream turbulence level exceeds 2%.

## Experimental Procedure and Measurement Techniques

The measurements were made at a nominal freestream velocity of 17.5 m/s for the three different temperature cases. The temperature difference was the difference between the mean plate surface temperature and the freestream temperature. Table 1 lists some parameters of interest at the measurement station.

### Velocity Profiles

Mean and fluctuating components of the streamwise velocity profiles were measured using hot-wire anemometry systems. A Thermo System Inc. (TSI) anemometer, model 1050, with a frequency response of 100 kHz was used. The anemometer was operated in constant-temperature mode at an overheat ratio of 1.8. A TSI standard single sensor boundary-layer probe, model 1218 T1.5, was used for both mean and fluctuating profile measurements.

The anemometer signal was processed through a low-pass filter, Krohn-Hite model 3323, with a cutoff frequency of 2,500 Hz, and then measured with an IBM AT personal computer and IBM DACA board data acquisition sytem. For each point of the velocity profiles, a total of 40,000 samples at a 10,000 Hz sampling rate were taken. This sampling frequency satisfies the Nyquist criteria for true rms measurements.[5] The cutoff frequency was determined after detailed analysis of the flow was made using Nicolet-660A digital spectrum analyzer.

### Turbulent Prandtl Number

Turbulent Prandtl number was calculated from the simultaneous measurements of the two components of the velocity and temperature at the same point in the flow. A subminiature TSI $x$ probe, model 1248-T1.5, and a subminiature TSI temperature probe, model 1276 P.5, were used for simultaneous measurements of $u$, $v$, and $T$. A special probe holder had to be designed and manufactured to hold both the $x$ probe and temperature probe. A total of 60,000 samples at 10,000 Hz were taken for each measuring quantity.

The effective measuring volume of the $\overline{u'T'}$ and $\overline{v'T'}$ measurements (the combined TSI subminiature $x$ probe model 1248 and TSI subminiature temperature probe model 1276) was 1.2 mm centerline to centerline. This distance represents a typical $\Delta z^+$ length of 50 wall units. Noting that the correlations of $R_{u,u}$ are similar in time-space characteristics to the $R_{T,T}$ correlations, then the $\overline{v'T'}$ measurements made (with the combined subminiature probes) have inherent uncertainties similar to standard $x$-probe measurements (not subminiature probes) of $\overline{u'v'}$. This is because $\overline{u'v'}$ uncertainties of the standard $x$ probe will be comparable to $\overline{u'T'}$ and $\overline{v'T'}$ uncertainties of the combined subminiature probes. This uncertainty should not be an area of major concern in quality of the data.

### Two-point Correlations

Two-point correlation measurements were made for the temperature fluctuations. Two temperature probes were positioned for known longitudinal distances between the two pro-

Table 1 Experimental parameters at the measurement station

| $\Delta T$, C | $x$, m | $Re_x \times 10^{-6}$ | $\delta$, mm | $\theta$, mm | $\delta_t$, mm | $Re_{\Delta 2}$ | $q_w$, $W$ |
|---|---|---|---|---|---|---|---|
| 10 | 2.45 | 2.84 | 45 | 4.7 | 38 | 3770 | 14.43 |
| 15 | 2.45 | 2.84 | 45 | 4.7 | 42 | 4540 | 21.50 |
| 20 | 2.45 | 2.84 | 45 | 4.7 | 45 | 4690 | 28.49 |

bes. One probe was held fixed at a given $y^+$ value and the other probe was moved to different longitudinal, $x^+$ positions for the same $y^+$ value. The reference heights for the streamwise correlation were set at $y^+$ values of 75, 175, and 425. For each height and each temperature difference case, a total of five $\Delta x^+$ values from 150 to 750 were measured. For every temperature probe and every measurement point, a total of 60,000 samples at a sampling rate of 10,000 Hz were taken. The cutoff frequency for both probes was set at 2000 Hz. A Cyborg ISAAC-2000 data acquisition system in conjunction with an IBM/AT personal computer was used for two-point correlation measurements.

## Uncertainty Analysis

The uncertainty caused by equipment accuracy and statistical calculations in this study was calculated. The standard approach presented by Kline and McClintock and described by Holman[6] was followed for uncertainty analysis of the mean quantities. The uncertainties were estimated with odds of 20:1. The statistical or random error uncertainties of the fluctuating quantities were estimated from the observed scatter in measurements as well as from the equations given by Bendat and Piersol.[5] Based on these estimates and the definition for turbulent Prandtl number, the uncertainty in $Pr_t$ was estimated from the root sum square combination of all the terms.[7] The results of the uncertainty analysis are listed in Table 2.

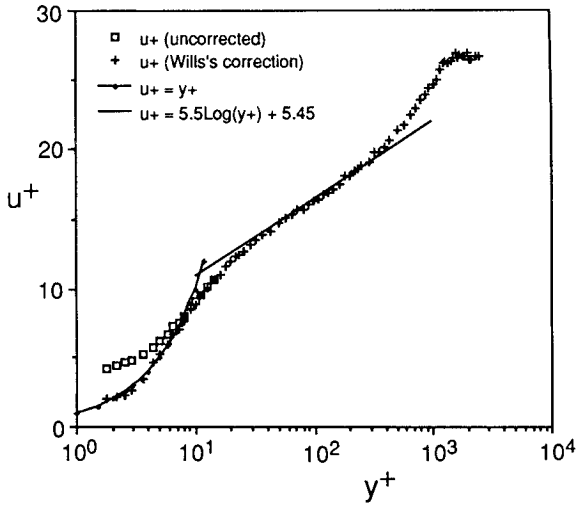


Fig. 5 Universal velocity-law-of-the-wall profile.

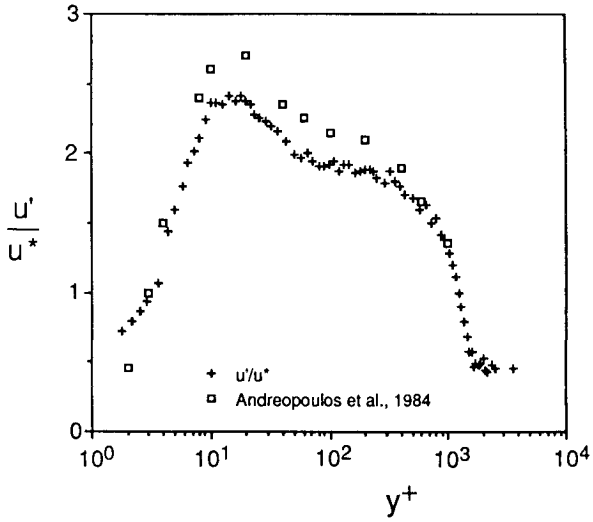


Fig. 6 Streamwise velocity fluctuations.

Table 2 Typical uncertainty estimates

| | |
|---|---|
| $U$ | ±1.7% |
| $u_{rms}$ | ±4.5% |
| $v_{rms}$ | ±5.3% |
| $u'v'$ | ±12.5% |
| $v'T'$ | ±14.2% |
| $u'T'$ | ±13.0% |
| $Pr_t$ | ±19.0% |
| $R_{T,T}$ | ±1.3% |

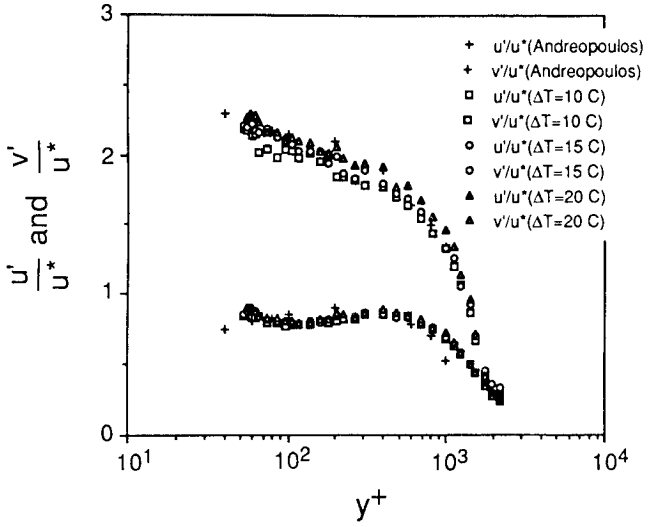


Fig. 7 Streamwise and normal velocity fluctuations.

## Presentation of Results

The streamwise velocity profile measurements were used to check the maturity and growth of the hydrodynamic boundary layer, and to determine the local friction coefficient distribution along the plate using the Clauser-chart method. Based on the velocity law-of-the-wall results, the characteristics of the boundary layer were found to be mature and normal at the stations at which the measurements were made. A typical universal mean velocity profile nondimensionalized with respect to the friction velocity is shown in Fig. 5. The near-wall region velocity data was corrected to account for the wall effects. Wills[8] correction method was used for the hot-wire data in the near-wall region. Corrections were applied up to a $y^+$ value of about 14. The Wills correction and the uncorrected data can be seen in Fig. 5. At a $y^+$ value of 14, virtually no effect of the heat-conducting wall was observed. The velocity data in the logarithmic core region fit very closely the law-of-the-wall equation given by Patel.[9] The spanwise velocity profile measurements were used to check the two-dimensionality of the flow. At the measurement station, 2.45 m from the leading edge, the maximum spanwise variation of velocity was less than ±1.5%, and occurred within the boundary layer where the local turbulence level was grater than 8%.

The longitudinal velocity fluctuations are shown in Fig. 6 as a function of logarithm $y^+$. In Fig. 6 the fluctuations have been nondimensionalized with wall variables and are compared with the data of Andreopoulos et al.[10] The maximum velocity fluctuation appears to be at a $y^+$ value of about 15 for both the present data, $Re_\theta = 4500$, and that of Andreopoulos et al., $Re_\theta = 5535$, with the maximum difference of about 9.4% at their peak values. Andreopoulos et al. have shown the Reynolds number dependence of the rms values of the longitudinal velocity fluctuations. Their results indicated that the peak rms values increase as Reynolds number is increased. Therefore, the higher peak value of the data of Andreopoulos et al. was due to the higher Reynolds number value.

Figure 7 shows the variation of the longitudinal and normal velocity fluctuations, normalized with respect to the friction

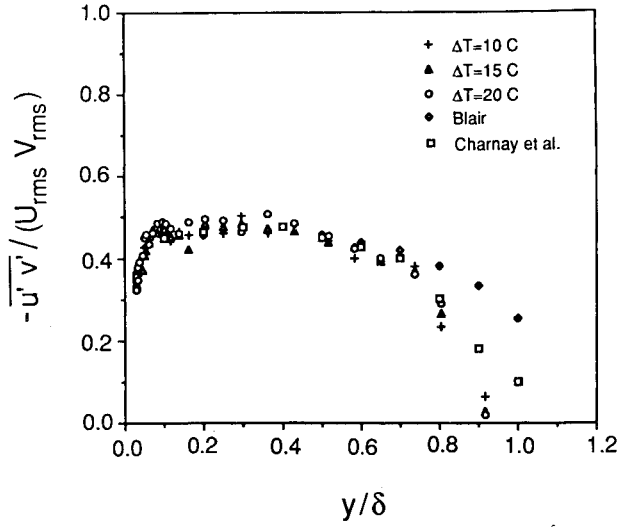


**Fig. 8 True time averaged shear stress profiles.**

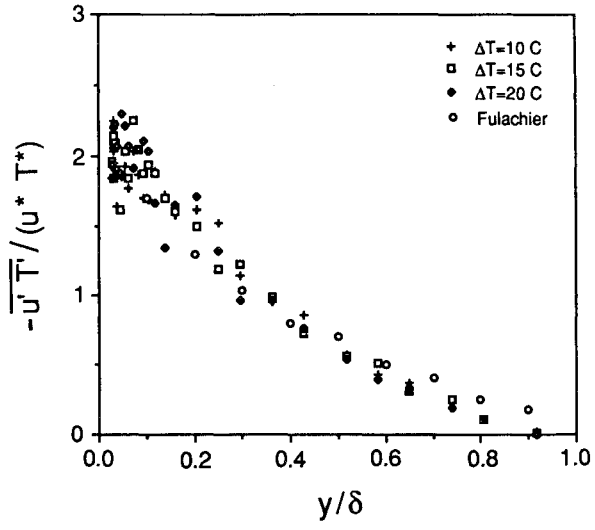


**Fig. 9 Longitudinal heat flux profiles.**

velocity, across the turbulent boundary layer for the three temperature difference cases. Since the freestream velocity was kept constant for all the three cases, it was expected that the streamwise, $u'$, and normal, $v'$, fluctuation profiles would be similar. Comparison of the three profiles shows that they are similar within 3%. Also on the same figure, the data of Andreopoulos[9] are shown. Andreopoulos studied the effect of Reynolds number on the characteristics of wall turbulence, and showed that the wall turbulence quantities are Reynolds number dependent. Comparison of the longitudinal fluctuations of the present data, $Re_\theta = 5450$, show close agreement to the Andreopoulos data to within ±2.5%. This comparison is better than the earlier comparison of the two profiles shown in Fig. 6, which was made at a $Re_\theta$ of 4500, suggesting a Reynolds number dependence of the streamwise fluctuations. The normal velocity fluctuation data also show reasonable agreement to the data of Andreopoulos, $Re_\theta = 3620$, the differences being largely due to the discrepancies in Reynolds number values.

### Turbulent Momentum and Heat Flux Measurements

From the simultaneous measurements of $u$,$v$, and $T$, the turbulence transport terms such as $\overline{u'v'}$, $\overline{u'T'}$, and $\overline{v'T'}$ were calculated. A total of 60,000 samples at 10,000 Hz were taken for each measured quantity. Each turbulence transport term was then determined from the simultaneous product of its two quantities.

Figure 8 shows the variation of the Reynolds shear stress terms across the boundary layer. The shear stress has been normalized with respect to the root mean square quantities. On the same figure, the data of Blair and Bennett[11] and Charnay et al.[12] are also shown. The agreement seems reasonable among the data. For $y/\delta > 0.8$, however, the Blair and Bennett data display some differences. Their data have larger values of $u'v'$ for $y/\delta > 0.8$ and do not approach zero as quickly as a function of height as the Charnay et al. data and the present data. Their data may have accounted for intermittency, whereas the present data do not.

Figure 9 shows the variation of the longitudinal heat flux across the boundary layer. The heat flux has been normalized with respect to the friction velocity and temperature and is plotted as a function of $y/\delta$ for the three temperature difference cases. On the same figure the data of Fulachier, given in Ref. 11, are shown. There is qualitative similarity between the two data. The scatter of the present data is observed mostly for $y/\delta$ values less than 0.3.

Figure 10 shows the variation of the normal heat flux across the boundary layer. The heat flux has been normalized with respect to the friction velocity and temperature, and is plotted as a function of $y/\delta$. On the same figure the data of Subramanian and Antonia[13] and Fulachier are shown. The data generally agree with each other. In the $y/\delta < 0.2$ region, the data show more scattered behavior, largely due to the high fluctuating structure of the flow in that region. In the $y/\delta > 0.2$ region, the agreement is better and the Subramanian and Antonia[13] data, the Fulachier data, and the present data are within ±7.5% of each other.

### Turbulent Prandtl Number

The turbulent Prandtl number is defined as the ratio of eddy viscosity $\epsilon_M$ to eddy conductivity $\epsilon_H$. Using the definitions for Reynolds shear stress and turbulent heat flux, given as

$$\tau_t = -\rho\overline{u'v'} = -\rho\epsilon_M \frac{\partial u}{\partial y}$$

$$q''_t = -\rho c_p \overline{v'T'} = -\rho c_p \epsilon_H \frac{\partial u}{\partial y}$$

the turbulent Prandtl number can be written as

$$Pr_t = \frac{\epsilon_M}{\epsilon_H} = \overline{u'v'}\,\frac{\partial T}{\partial y} \Big/ \left(\overline{v'T'}\,\frac{\partial u}{\partial y}\right)$$

Various assumptions have been made about the ratio of eddy viscosity to eddy conductivity, and several expressions have been proposed in attempts to predict the mean temperature

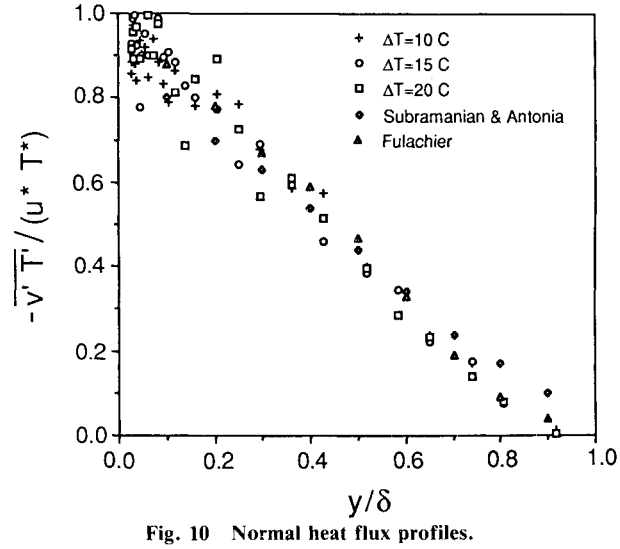


**Fig. 10 Normal heat flux profiles.**

profile and the average heat transfer coefficient in the boundary layer. The simplest one of all is the Reynolds analogy, which implies a turbulent Prandtl number having a value of unity. The assumption is that the momentum and heat are transported by similar processes, which leads to the same values for the eddy viscosity and conductivity for zero-pressure-gradient incompressible flow.

Experimental data have shown that the turbulent Prandtl number varies through the layer in a way that depends on both molecular Prandtl number and the flowfield. Measurements have shown that the wall region is characterized by values of the turbulent Prandtl numer slightly higher than unity, falling to less than one in the outer region.[7] In the logarithmic region, a number of experiments have shown that the turbulent Prandtl number value for zero-pressure-gradient flows, having air as working fluid, is approximately 0.9.[14,15] Rotta[16] presented an expression for $Pr_t$ as a function of $y/\delta$ in the outer region:

$$Pr_t = 0.9 - 0.4\,(y/\delta)^2$$

This expression indicates that $Pr_t$ has a uniform value of about 0.9 near the wall, and approaches to a value of about 0.5 at the edge of the boundary layer.

Launder,[17] in his review of the modeling of turbulent heat and mass transfer processes, pointed out that the work of many researchers leads to the conclusion that the turbulent Prandtl number is not constant across the boundary layer. He indicated that in the region of $10<y^+<35$ the turbulent Prandtl number is actually greater than 1. This result also is supported by the data of Blackwell et al.[15]

In further support of Launder's observation on the variability of the $Pr_t$ across the boundary layer, the results of Simpson et al.[14] indicate that the $Pr_t$ peaks at some $y^+<30$ and levels out to a nominal value between 0.8 and 1.0 for $100<y^+<1000$. For $y^+<10$, the results of Simpson et al.[14] showed different $Pr_t$ profiles that in some cases decreased below 1.0 and in others continued to peak. Based on these results, they defined an uncertainty envelope for the turbulent Prandtl number.

The results of the turbulent Prandtl number variation for the present study for the three temperature difference cases are shown in Fig. 11 as a function of $y^+$. The turbulent Prandtl number was evaluated from direct measurements of the Reynolds shear stress $\overline{u'v'}$ and simultaneous direct measurements of the normal heat flux $\overline{v'T'}$ across the boundary layer. The velocity gradient $\partial u/\partial y$ and the temperature gradient $\partial T/\partial y$ were obtained from the mean velocity and mean temperature profiles, respectively. On the figure, the uncertainty envelope determined by Simpson et al.[14] is shown. The comparisons in Fig. 11 show that the present data, with the exception of some points, fall within the uncertainty envelope of Simpson et al. For all the three temperature difference cases, the turbulent Prandtl number drops sharply from a peak value of about $1.35\pm0.05$ at a $y^+$ value of about 60 to a value of about 1, and then gradually decreases to a value of about $0.6\pm0.05$ close to the boundary-layer edge. Simpson et al. indicated that the $Pr_t$ peaked at $y^+<30$. The present data contain turbulent Prandtl number variations for $y^+>50$. Therefore, the Simpson et al. observation could not be compared to the present data.

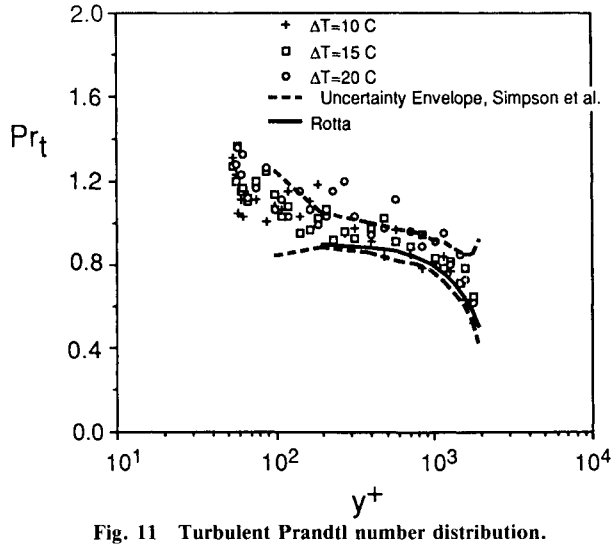


**Fig. 11 Turbulent Prandtl number distribution.**

Rotta's expression is also shown in Fig. 11. As seen in the figure the expression follows closely the lower curve of the uncertainty envelope. The agreement between the Rotta expression and the present data in the outer region appears to be reasonable, especially for the temperature differences cases of 10 C and 15 C. The Rotta expression drops to a value of 0.5 close to the boundary-layer edge, compared to a value of $0.6\pm0.05$ for the present data.

The present turbulent Prandtl number distribution across the boundary layer seems to support the distribution of the $Pr_t$ in the near-wall and outer-wall regions of the previous experimental measurements.[7,15] The near-wall region is characterized by values of the $Pr_t$ greater than unity, falling to approximately 0.6 in the outer edge of the boundary layer. It should, however, be mentioned that the uncertainty in turbulent Prandtl number calculation is $\pm19\%$, due to high uncertainty values in the calculation of $\overline{u'v'}$ and $\overline{v'T'}$ terms.

### Correlation Measurements

Two temperature fluctuation probes were used to measure the temperature fluctuations simultaneously at two streamwise locations. The turbulent signals from the two probes were then obtained and correlated for the three temperature difference cases.

The temperature cross-correlation coefficient is defined as

$$R_{T,T} = T(x,y,z,t)T(x+\Delta x, y+\Delta y, z+\Delta z, t+\Delta t)\,/$$

$$[T_{\rm rms}(x,y,z)T_{\rm rms}(x+\Delta x, y+\Delta y, z+\Delta z)]$$

where $T$ represents the temperature fluctuations; $T_{\rm rms}$ is the root mean square value of $T$, $(x,y,z)$ is the location of one probe in space, $(\Delta x,\Delta y,\Delta z,)$ is the separation of the second probe from the first probe, $t$ is the time coordinate, and $\Delta t$ is the variable time shift. This cross-correlation coefficient is a measure of the similarity between the two temperature fluctuation signals. The extent of similarity between the two signals depends on the absolute value of the cross-correlation coefficient. A high absolute value means that the two signals are highly correlated and are similar.

### Convection Velocity

The mean convection velocity of the temperature fluctuations was obtained from the correlation measurements in the streamwise direction ($\Delta y=\Delta z=0$). Two temperature probes were positioned at different streamwise spacings and the same heights. The reference heights were set at $y^+$ values of 75, 175, and 425 to get a distribution of the mean convection velocity of the $T'$ structure. For each height and each temperature difference case, a total of five $\Delta x^+$ values were taken. The space-time correlations of temperature fluctuations for the $\Delta T=15$ C case and the three reference heights are shown in Figs. 12a-c. Each figure contains the space-time correlations at the same height and different streamwise spacings between the probes.

From the space-time correlation measurements, the time shifts of the peak $R_{T,T}(\Delta x^+)$ correlation values from the zero time axis were measured for the three temperature difference cases. These shifts are imposed by the passage of turbulent temperature fluctuation eddies that move with a convection

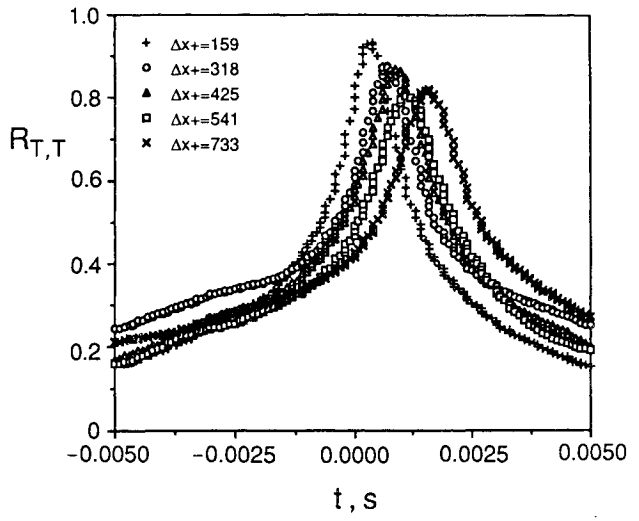


**Fig. 12a Determination of the mean convection velocity: $\Delta T = 15°$ C, $y^+ = 75$.**

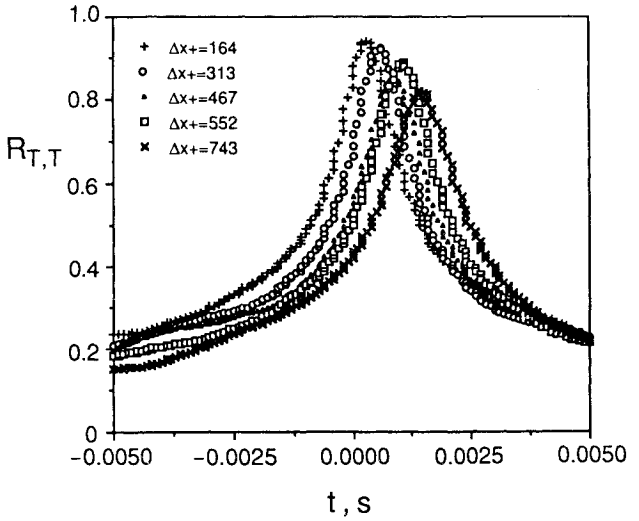


**Fig. 12b Determination of the mean convection velocity: $\Delta T = 15°$ C, $y^+ = 75$.**

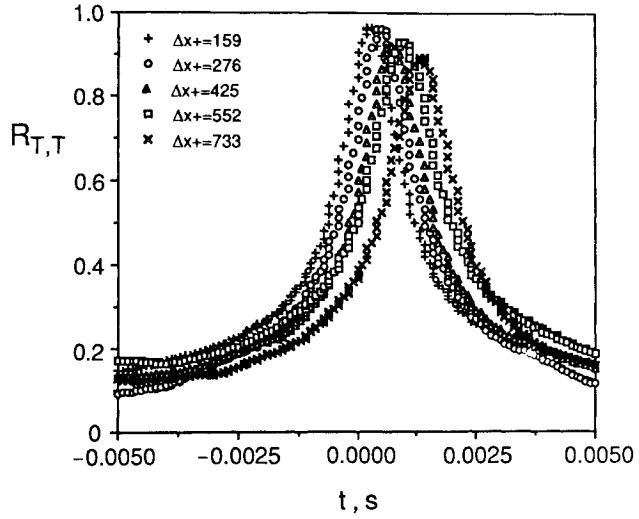


**Fig. 12c Determination of the mean convection velocity: $\Delta T = 15°$ C, $y^+ = 75$.**

velocity that is a fraction of the freestream velocity. The results of the temporal displacement vs the spatial displacement are shown in Fig. 13 for the three heights. Each curve contains the results of the three temperature difference cases. The temporal displacements vary linearly with the streamwise separation and appear to be independent of the temperature difference. The slope of each line, $dx/dt = U_c$, gives an estimate of the convection velocity of the temperature fluctuations at the given height.

Figure 14 shows the variation of the mean convection velocity with height. On the same figure, the local mean velocity is also shown. The convection velocity of $T'$ structure varies approximately from $0.65u_\infty$ at $y^+ = 75$ to $0.77u_\infty$ at $y^+ = 425$. For the isothermal turbulent boundary-layer flow, Strataridakis et al.[2] measured the convection velocities of the $u'$, $v'$, and $u'v'$ structures. For the convection velocity of the $u'$ structure, they reported variations approximately from $0.25u_\infty$ at $y^+ \approx 12$ to $0.8u_\infty$ at $y^+ \approx 150$. For the convection velocity of the $v'$ and $u'v'$ structures, they found that the convection velocity of both structures remains invariant with height and is equal to $0.80u_\infty$. The convection velocity of the $u'$ structure of the Strataridakis et al. data is equal to 25% of the freestream at $y^+ \approx 12$. The lowest height considered in the present study for the evaluation of the convection velocity was at $y^+ = 75$, which resulted in a $T'$ structure convection velocity of 65% of the freestream. The Strataridakis et al. data for the $u'$ structure convection velocity reached 80% of the freestream at $y^+ \approx 150$. This 80% value is believed to be the maximum percentage of the freestream velocity reported in studies made on isothermal turbulent boundary-layer flows. The convection velocity of the $T'$ structure of the present study

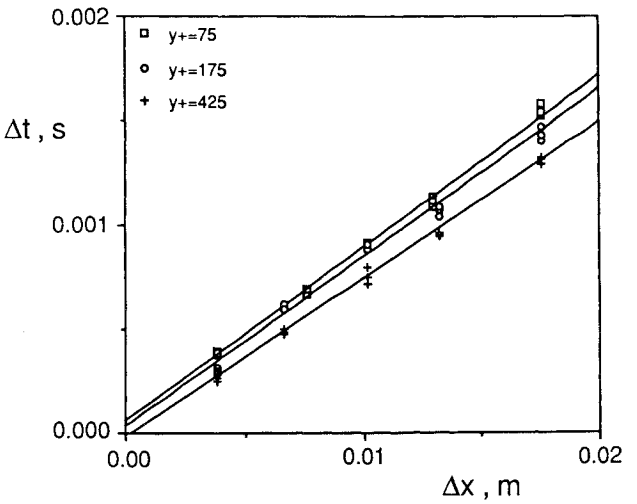


**Fig. 13 Temporal displacement vs spatial displacement.**

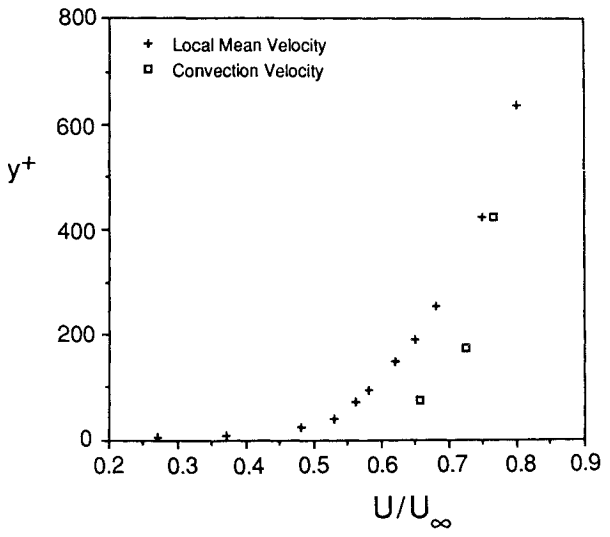


**Fig. 14 Variation of the mean convection velocity.**

reached 77% of the freestream velocity at $y^+ = 425$, which is higher than the corresponding level of the $u'$ structure.

It is felt that the difference in mean convection speed between $0.65u_\infty$ at $y^+ = 75$ and $0.77\ u_\infty$ at $y^+ = 425$ is significant, as it suggests a decreasing convection speed with decreasing height. It is, however, not known from the data available whether the convection speed as a function of height follows the $u'$ structure, or if it follows a mixed-mode behavior between the $u'$ and $v'$ structures. However, since the uncertainties of the cross-correlation technique and the $\Delta x$ vs $\Delta t$ slope are small, the mean convection speed does appear to vary as a function of height, and does not oscillate about a constant value throughout the boundary layer. Thus, the convection speed of the $T'$ structure is not constant and appears to increase in speed as distance away from the wall increases. The exact nature of the function is not known due to the lack of sufficient experimental data. The limited data trend, however, does suggest it follows a curve similar to the mean convection velocity of the $u'$ structure, although it is inconclusive to state that the $T'$ convection speed function exactly follows the $u'$ convection speed function.

## Conclusions

Turbulent Prandtl numbers profiles for the three temperature difference cases were determined to fall in the uncertainty envelope determined by Simpson et al.[14] The near-wall region was characterized by values of the turbulent Prandtl number greater than unity, falling to approximately 0.6 in the outer edge of the boundary layer. The profiles were determined from the simultaneous measurements of $u$, $v$, and $T$ at the same points in the turbulent boundary layer, which resulted in the determination of the turbulent Prandtl number from a totally direct measurement.

For the first time, from the space-time correlations of the temperature fluctuations, the mean convection velocity of the large-scale structure of the turbulent temperature fluctuations was determined for the three temperature difference cases.

The mean convection velocity of the temperature fluctuation structures was determined to vary from $0.65u_\infty$ at $y^+ = 75$ to $0.77u_\infty$ at $y^+ = 425$, and appeared to be independent of the temperature difference cases considered in this study. The convection velocity of the $T'$ structure is not constant across the boundary layer, and appears to increase as the distance away from the wall increases. The exact functional form is not known, due to the lack of sufficient experimental data.

## References

[1]Kline, S. J., and Robinson, S. K., "Quasi-Coherent Structures in the Turbulent Boundary Layer: Part I. Status Report on a Community-Wide Summary of the Data," Zoran P. Zaric' Memorial International Seminar on Near-Wall Turbulence, Dubrovnik, Yugoslavia, May 16-20, 1988.

[2]Strataridakis, C. J., White, B. R., Robinson, S. K., "Experimental Measurements of Large Scale Structures in an Incompressible Turbulent Boundary Layer Using Correlated X-Probes," AIAA Paper 89-0133, 1989.

[3]Berukhim, A., "Heat Transfer Measurements in Turbulent Boundary Layer," M.S. Thesis, Univ. of California, Davis, CA 1986.

[4]Blair, M. F., "Influence of Free-Stream Turbulence on Turbulent Boundary Layer Heat Transfer and Mean Profile Development, Part I-Experimental Data," *Journal of Heat Transfer*, Vol. 105, No. 1, 1983, pp. 33-40.

[5]Bendat, J. S., and Piersol, A. G., *Random Data,* 2nd ed. Wiley Interscience, 1986.

[6]Holman, J. P., *Experimental Methods for Engineers*, 3rd Ed., McGraw-Hill, New York, 1978.

[7]Orlando, A. F., Moffat, R. J., and Kays, W. M., "Turbulent Transport of Heat and Momentum in a Boundary Layer Subject to Deceleration, Suction and Variable Wall Temperature," Rep. HMT-17, Thermosciences Div., Dept. of Mechanical Engineering, Stanford Univ., Stanford, CA, 1974.

[8]Wills, J. A. B., "The Correction of Hot-Wire Readings for Proximity to a Solid Boundary," *Journal of Fluid Mechanics,* Vol. 12, Pt. 3, 1962, pp. 388-398.

[9]Patel, V. C., "Calibration of the Preston Tube and Limitations on its Use in Pressure Gradients," *Journal of Fluid Mechanics*, Vol. 23, Pt. 1, 1965, pp. 185-208.

[10]Andreopoulos, J., Durst, F., Zaric, Z., and Jovanovic, J., "Influence of Reynolds Number on Characteristics of Turbulent Wall Boundary Layers," *Experiments in Fluids*, Vol. 2, No. 1, 1984, pp. 7-16.

[11]Blair, M. F., and Bennett, J. C., "Hot-Wire Measurements of Velocity and Temperature Fluctuations in a Heated Turbulent Boundary Layer," *Journal of Heat Transfer,* Vol. 104, No. 2, 1982, pp. 271-279.

[12]Charnay, G., Mathhieu, J., and Comte-Bellot, "Response of a Turbulent Boundary Layer to Random Fluctuations in the External Stream," *Physics of Fluids*, Vol. 19, No. 9, pp. 1261-1272.

[13]Subramanian, C.S., and Antonia, R.A., "Effect of Reynolds Number on a Slightly Heated Turbulent Boundary Layer," *International Journal of Heat Mass Transfer*, Vol. 24, No. 11, 1981, pp. 1833-1981.

[14]Simpson, R. L., Whitten, D. G., and Moffat, R. J., "An Experimental Study of the Turbulent Prandtl Number or Air with Injection and Suction," *International Journal of Heat and Mass Transfer,* Vol. 13, No. 1, 1970, pp. 125-143.

[15]Blackwell, B. F., Kays, W. M., and Moffat, R. J., "The Turbulent Boundary Layer on a Porous Plate: An Experimental Study of the Heat Transfer Behavior with Adverse Pressure Gradients," Rept. HMT-16, Thermoscience Div., Dept. of Mechanical Engineering, Stanford Univ., Stanford, CA, 1972.

[16]Rotta, J. C., "Turbulent Boundary Layers in Incompressible Flows," *Progress in Aeronautical Sciences,* edited by A. Ferri, D. Kuchemann, and L. Sterne, Vol. 2, Pergamon, New York, 1962, pp. 1-219.

[17]Launder, B. E., "Heat and Mass Transport," *Topics in Applied Physics: Turbulence,* Vol. 12, edited by P. Bradshaw, Springer-Verlag, New York, 1978, pp. 232-287.